Geomorphology 246 (2015) 305–320

Contents lists available at ScienceDirect

Geomorphology

journal homepage: www.elsevier.com/locate/geomorph

Fluvial islands: First stage of development from nonmigrating (forced) bars and woody-vegetation interactions

Coraline L. Wintenberger [a], Stéphane Rodrigues [a,c,*], Jean-Gabriel Bréhéret [a], Marc Villar [b]

[a] Université François Rabelais de Tours, E.A. 6293 GéHCO, GéoHydrosystèmes Continentaux, Faculté des Sciences et Techniques, Parc de Grandmont, 37200 Tours, France
[b] INRA, UR 0588, Amélioration, Génétique et Physiologie Forestières, 2163 Avenue de la Pomme de Pin, CS 40001 Ardon, 45075 Orléans, Cedex 2, France
[c] Université François Rabelais de Tours, UMR CNRS 7324 CITERES, CItés, TERritoires, Environnement et Sociétés, 33-35 allée Ferdinand de Lesseps, 37000 Tours, France

ARTICLE INFO

Article history:
Received 8 October 2014
Received in revised form 15 June 2015
Accepted 19 June 2015
Available online xxxx

Keywords:
Populus nigra
Bars
Island
Sandy–gravelly rivers

ABSTRACT

Fluvial islands can develop from the channel bed by interactions between pioneer trees and bars. Although vegetation recruitment and survival is possible on all bar types, it is easier for trees to survive on nonmigrating bars developed from a change in channel geometry or to the presence of a steady perturbation. This field study details the first stages of development of a vegetated mid-channel, nonmigrating (or forced) bar and its evolution toward an island form. Over six years, analysis of bed topographical changes, vegetation density and roughness, scour and fill depths, sediment grain size and architecture, and excess bed shear stress highlighted a specific signature of trees on topography and grain size segregation. Two depositional processes combining the formation of obstacle marks and upstream-shifting deposition of sediments led to the vertical accretion of the vegetated bar. During the first stage of the bar accretion, bedload sediment supply coming from surrounding channels during floods was identified as a key process modulated by the presence of woody vegetation and a deflection effect induced by the preexisting topography. Grain size segregation between vegetated and bare areas was also highlighted and interpreted as an important process affecting the development of surrounding channels and the degree of disconnection (and hence the speed of development) of a growing island. The heterogeneity of bedload supply can explain why sediment deposition and density of trees are not strictly related. A general conceptual model detailing the first stages of evolution from a bar to an established island is proposed for relatively large lowland rivers.

1. Introduction

Fluvial vegetated islands are key components of fluvial systems as they influence the planform (Tal and Paola, 2007; Gibling and Davies, 2012; Gibling et al., 2014; Ielpi et al., 2014) and the biodiversity of these hydrosystems (Corenblit et al., 2014). Processes involved in their creation participate to the morphological evolution of multiple-channel rivers as well as sediment archiving. Although many studies have been carried out on the interactions between woody vegetation and sedimentary processes in alluvial rivers (McKenney et al., 1995; Nanson and Knighton, 1996; Abbe and Montgomery, 2003; Gurnell et al., 2005, 2012; Corenblit et al., 2009), investigations carried out on the zone of intense interactions between plants and physical processes (active part of the channel) remain rare (see Corenblit et al., 2011; Fig. 3 in Gurnell et al., 2012). Specifically, for mid-channel bars, the first steps of evolution from the bar state to the island state are not known in terms of velocity, sedimentary processes involving young pioneer woody vegetation, and vertical/lateral accretion rates under quasi-unlimited sediment supply conditions.

From a morphological perspective, excluding sedimentary processes and botanical specificities, a fluvial island was defined by Osterkamp (1998, pp. 530–531) as 'geomorphic feature surrounded by channel, that is higher than mean water level (or the principal network of adjacent ephemeral or intermittent stream channels) and that persists sufficiently long to permit the establishment of a permanent vegetation cover if adequate moisture is available'. However, and as stated by Brice (1964) and Bridge (2003, p. 149), the distinction between vegetated bars and islands remains an issue; specifically, mid-channel bars were defined as unvegetated and submerged at bankfull flow (Drago et al., 2008), whereas islands emerge under these flow conditions. As shown by Osterkamp (1998) and Gurnell et al. (2001), established fluvial islands can result from several processes among which excision of floodplain deposits or building involving dead or living woody vegetation present on channel bars (Osterkamp, 1998; Kollmann et al., 1999; Gurnell et al., 2001, 2012; Nakayama et al., 2002; Bertoldi et al., 2011; Mikuś et al., 2013). For this latter case, the regeneration process of vegetation on flow resistance and sediment deposition influences the island creation: sprouting from living driftwood exerts a rapid and strong feedback on physical parameters whereas seedling impact is reduced during their first stage of development (Moggridge and Gurnell, 2009).

* Corresponding author.
E-mail address: srodrigues@univ-tours.fr (S. Rodrigues).

http://dx.doi.org/10.1016/j.geomorph.2015.06.026
0169-555X/© 2015 Published by Elsevier B.V.

Woody pioneer vegetation can recruit or sprout on two general types of alluvial bars, namely free (or migrating) and forced (nonmigrating) bars (see review in Rodrigues et al., 2015). Nonmigrating bars (e.g., point bars, mid-channel bars) correspond to sediment accumulation developing due to a discontinuity in the channel geometry (Olesen, 1984; Struiksma et al., 1985; Parker and Johanneson, 1989; Crosato et al., 2011), while free bars arise because of morphodynamic instability (Tubino, 1991; Tubino et al., 1999). Since the latter are rather unstable and rapidly migrating units (Claude et al., 2014), the development of vegetation and its resistance to physical stresses on these macroforms is rare. Contrarily, because of their conditions of formation, nonmigrating bars are relatively stable units on which woody vegetation can recruit and survive even in morphologically very active rivers (Nakayama et al., 2002; Charron et al., 2011; Crouzy et al., 2013). Large woody debris and vegetation can sometimes trigger a local nursing effect interesting for the development of other seedlings (Gurnell et al., 2005).

Once established on bars, the permeable obstacle constituted by the vegetation influences their morphological development by increasing flow resistance (McKenney et al., 1995; Fathi-Maghadam and Kouwen, 1997; Darby and Simon, 1999; Freeman et al., 2000; Antonarakis et al., 2010), decreasing flow velocity (Li and Shen, 1973; Wu et al., 1999; Copeland, 2000), and enhancing deposition and fixing of sediments (Graf, 1978; Fielding et al., 1997; Wende and Nanson, 1998; Kollmann et al., 1999; Gurnell et al., 2001; Nakayama et al., 2002; Francis et al., 2006; Euler and Herget, 2012; Euler et al., 2014; Manners et al., 2014). More specifically, the presence of shrubs and trees often creates obstacle marks (horseshoe scour hole, sediment ridge) which constitute a first step in the metamorphosis process from a bar to an island (Nakayama et al., 2002; Rodrigues et al., 2007; Euler et al., 2014). As a consequence of merging of these obstacle marks and vertical accretions, the morphology of bars evolves from a relatively flat bed to a ridge-and-swale topography. This process induces a biotic signature in the bar topography as shown by Bertoldi et al. (2011) for the Tagliamento River. At this stage, the increase of the deflection power of tree bands, the decrease in flooding duration of the bar, and its progressive disconnection from surrounding channels induces a decrease in sediment supply (in terms of quantity and grain size). As a consequence, deposition of small quantities of fine sediments mainly transported as suspended and washloads and a smoothing of the bar/island topography is observable (Rodrigues et al., 2007). Anyway, the time needed to create a fluvial island (see definition above) from a mid-channel nonmigrating bar has never been documented.

This paper focuses on the first stage of development of an island from a mid-channel, nonmigrating bar of the River Loire colonized by the black poplar (*Populus nigra*, L). This tree species has been recognized to modify its physical environment and the riparian community structure, function, resistance, and resilience (see review by Corenblit et al., 2014). Detailed surveys conducted over six years on channel bed topography, scour-and-fill processes, sediment grain size evolution, and physical features of in-channel woody vegetation are presented. In terms of chronology of floodplain development, this study covers stages 1 (active river bed), 2 (stabilizing bar), and 3 (incipient floodplain) as proposed by Reinfelds and Nanson (1993). In terms of fluvial biogeomorphological succession (Corenblit et al., 2014), it corresponds to the pioneer and biogeomorphological stages.

The general scientific goal addressed here concerns the mechanistic understanding of the first stages of evolution of an island from a mid-channel bar where woody pioneer vegetation recruited. Specifically, the time needed to create a fluvial island from a mid-channel, nonmigrating bar is documented. More precisely, the paper addresses the following points:

- How the tree signature in the topography of a bar evolves since the year of recruitment;
- To what extent bedload sediment supply affects the morphological evolution of the vegetated bar; and
- We propose a conceptual model of the evolution of a mid-channel bar to an island for large sand- and gravel-bed rivers. In our model we identify those variables important for the morphological evolution of a bar to an island, specifically highlighting the influence of vegetation on sediment archiving.

2. Material, methods and study site

2.1. Loire River islands

The Loire River drains a watershed of 117,000 km^2 that experiences an irregular flow regime. Floods are caused by storms occurring in the upstream part of the river during winter and spring (Dacharry, 1996; Duband, 1996) and by intense rainfall coming from the Atlantic Ocean. The Loire has been heavily influenced by human activities such as damming, embanking, building of groynes for navigation, and intense sediment mining that stopped in 1995 (Latapie et al., 2014). The resulting incision of the main channel and the end of pasture activity triggered a development of woody pioneer vegetation as well as a rapid morphological evolution of the river from an island-braided to anabranching style.

The recent incision of the main channel in the last 50 years has led to significant channel bank erosion (Latapie et al., 2014), adjustment of secondary channels (Rodrigues et al., 2006), and island width by inducing bank retreat (Gautier and Grivel, 2006; Détriché et al., 2010).

In the middle reaches of the Loire, established islands are covered by forested areas or former pastures where fine sediments, potentially affected by polymetallic contamination (Grosbois et al., 2012; Dhivert et al., 2015), settle during floods. Trenches made on the banks of these islands show a typical stratigraphical sequence, comparable to some extent to gravel-bed rivers, made of two main units developed on several metres (3 to 5 m usually) above the low flow water level. Typically, the basal unit was deposited briefly as channel deposits and covered by a finer unit composed by suspended sediments deposited over long time periods.

2.2. Study site

The site of Mareau-aux-Prés is located near Orléans in the middle reaches of the Loire, about 1.2 km from the confluence of the Loire and the Loiret rivers. In this area the bedrock consists of Tertiary lacustrine limestone overlaid with the siliceous sediments of the Loire coming from the upper reaches. Outcrops of the bedrock can appear in the main channel caused by intense past sediment mining (Fig. 1; Latapie et al., 2014).

In this area the river is characterized by a low amplitude meander planform combined with a large cross section (embanked width ranges from 370 m upstream to 760 m downstream the study site). The average channel slope in the study reach is 0.000226 m$\cdot$m^{-1} and mean annual discharge equals 344 m$^3\cdot$s^{-1} (gauging station of Orleans, 10 km upstream). The specific stream power at bankfull flow equals 22 W$\cdot$m^{-2} (see Latapie, 2011; and Fig. 9 in Latapie et al., 2014).

Several islands of different ages and sizes are present in this sinuous part of the river. These islands developed in the past from a colonization by woody vegetation of previously existing bars mentioned on the map of 1848 (Fig. 1A). The presence of those bars is associated with the lee effect provided by the presence of the bedrock that appears just upstream of the study site. This riffle is also responsible for the increase in width of the cross section resulting in a decrease in sediment transport capacity (Wintenberger, 2011).

Before 1989, an island was present at the location of the bar (remnants of this island, located NW from the bar is visible in 2010); this island has been partially eroded. Basically, the whole bar appeared in its current form in years 2003 and 2004 (Fig. 1).

The bar studied has a triangular planform (with an area of ca. 20,000 m^2 and length of 260 m); its average elevation equals 84.5 m asl

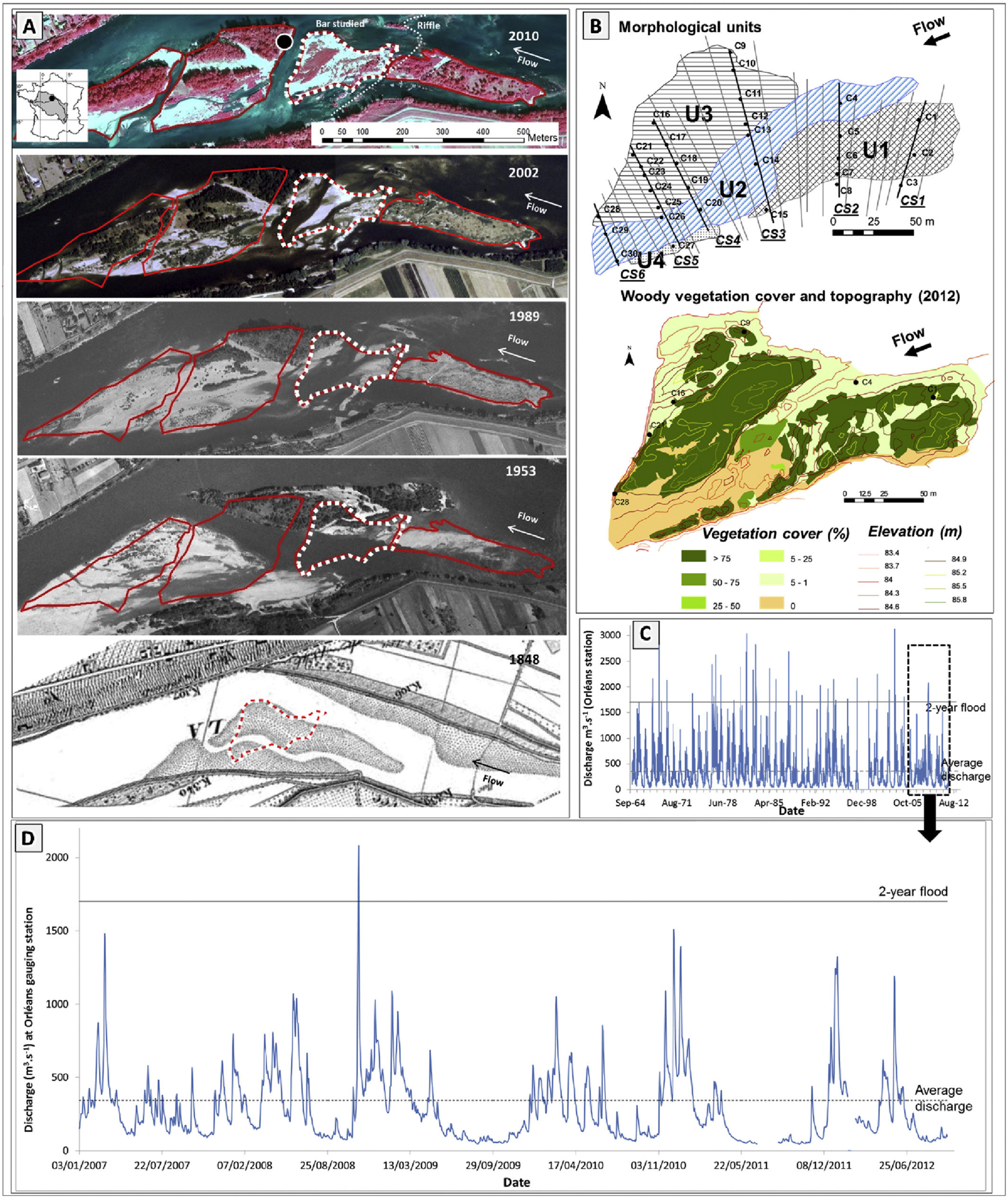

Fig. 1. Location of the study site of Mareau-aux-Prés. A regional view of the site is available from Google Earth (47°51′50.90″N, 1°46′59.92″E). (A) Morphological evolution of the study site between 1848 and 2010 (photo courtesy of DREAL Centre, IGN, and Richard Chevalier, IRSTEA). The black point on the aerial photograph of 2010 and the dotted lines correspond to the trench presented in Fig. 2B and to the bar studied respectively. (B) Morphological units of the bar, location of the cross sections surveyed (grey lines) and coupled with scour chains (black lines and points). (C,D) Hydrograph of the Loire between 1965 and 2012 (C) and during the study period (D).

(above sea level). The sediments consist mainly of a mixture of siliceous particles ranging from pebbles to fine sands even if some flint cobbles resulting from the weathering of the calcareous bedrock are present. Armour layers are located between vegetation patches while finer sediments are located in the tree bands.

In 2004, the bar was colonized by seedlings that developed into a very dense stand of *P. nigra* L. between 2005 and 2012 (Villar, 2011). As commonly seen on the Loire, the preservation potential of this type of vegetation is very high: if no important stress (flood, severe drought) occurs during the first year of development, this type of vegetation will not be removed even for very high magnitude floods. Other species such as *Salix purpurea* L. and *Acer negundo* L. were present but very rare. *Carex* spp. were sparsely distributed on the margins of the bar.

Vegetation bands developed on four morphological units were distinguished on the bar since the beginning of the study in 2007 (Fig. 1B). Units 1, 3, and 4 correspond to very dense tree bands, whereas unit 2 is a chute channel located at lower elevation and submerged during medium to low flows. Coarse sediments, namely pebbles and cobbles, are located in unit 2 while sands and gravels dominate units 1, 3, and 4.

Between 1965 and 2012, the highest discharge recorded was equal to 3230 $m^3 \cdot s^{-1}$ and occurred in December 2003. During this time period the 2-year flood was reached 31 times. Between 2007 and 2012, the average discharge value (344 $m^3 \cdot s^{-1}$) was exceeded 31% of the time. Only one flood event (November 2008, maximum discharge recorded equal to 2080 $m^3 \cdot s^{-1}$) exceeded the 2-year flood discharge (1700 $m^3 \cdot s^{-1}$). No

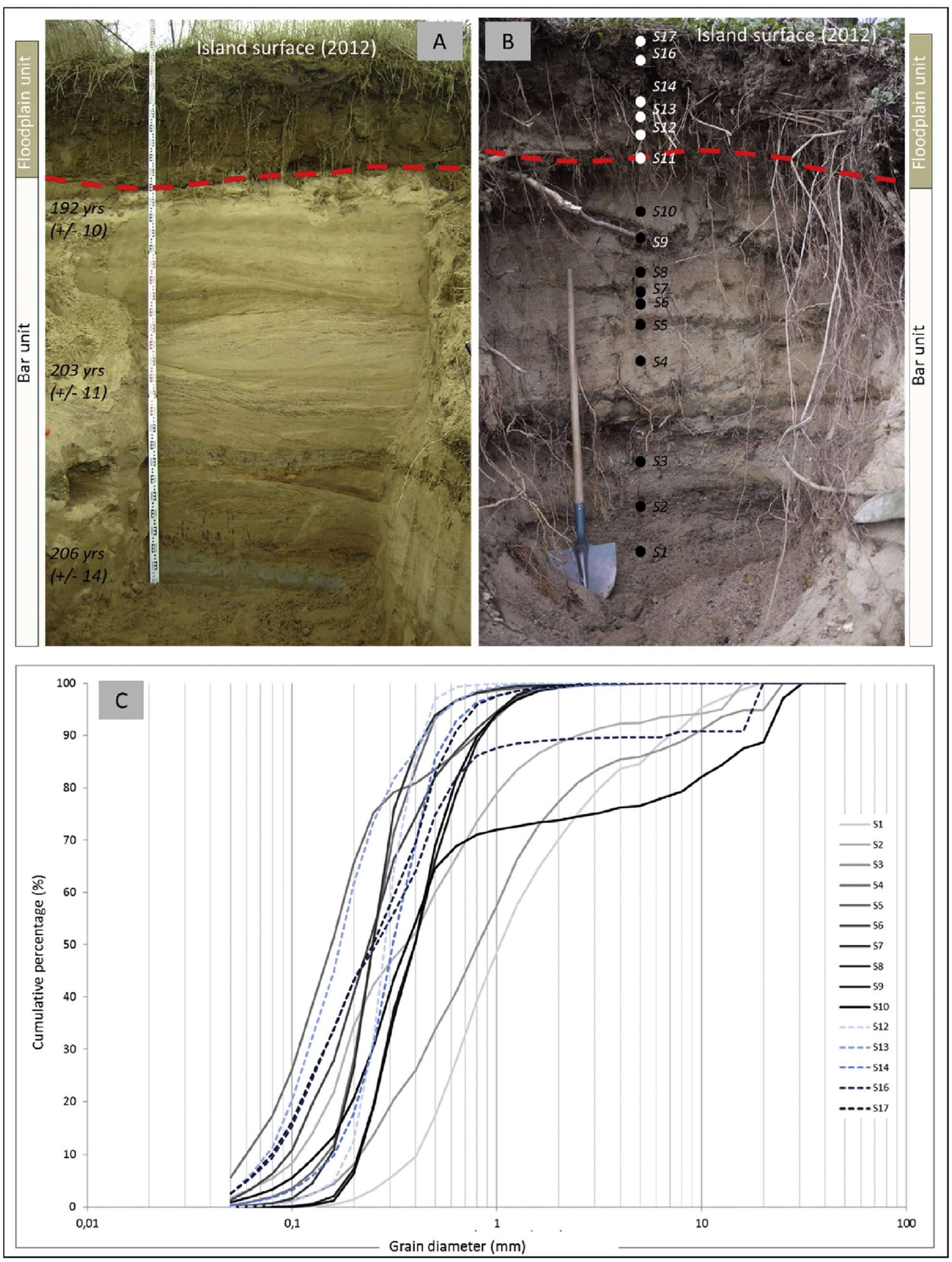

Fig. 2. Typical stratigraphy of islands of the middle reaches of the Loire River. Trenches dug on two islands located in the study sites of Bréhemont (A, see Detriché et al., 2010, for details) and Mareau-aux-Prés (B) located (respectively) 800 and 648 km from the sources. For the site of Bréhémont, OSL datings were performed. (C) Corresponds to cumulative curves of the sediments of the trench presented in (B).

flood peak reached the 5-year flood (2300 $m^3 \cdot s^{-1}$), and 11 flood peaks equal to 1000 $m^3 \cdot s^{-1}$ occurred in Orléans (Fig. 1D).

2.3. Topographical survey

Between 2007 and 2012, the bar topography was annually surveyed with a centimetrical accuracy using a Trimble M3 total station and a Magelan Proflex 500 DGPS.

A total of 25 cross sections located 10 m apart in average were surveyed (Fig. 1B). As recommended by Heritage et al. (2009), additional points were surveyed on the bar at morphological outlines, slope breaks, and cut banks to reduce error during the construction of digital elevation models (DEMs). The number of points recorded during measurements reached a maximum of 8299 points and varied according to the emerged surface of the bar; density of survey points on the bar was 1 point per 7.7 m^2 on average.

LiDAR data provided by the DREAL Centre in 2003 (measurements made during low flows) were also analysed. The measurements were not strictly located on the above-mentioned cross sections but were useful to determine the morphology of the bar 2 years before vegetation recruitment.

All the points acquired during the field surveys were combined to create DEMs using the linear interpolation TIN (Triangular Interpolation Network) function of ArcGIS 10 software. This interpolator was demonstrated to be a reliable tool to describe the morphology of alluvial bars (Moore et al., 1991; Fuller and Hutchinson, 2007). The DEMs were compared to obtain sediment balance, slope maps, and eroded/deposited volumes using the Spatial Analyst function of ArcGIS 10. The LiDAR data were not compared in terms of sediment balance since the bar was smaller in 2003 (ca. 11,800 m^2).

Because the data sets differed in sample size, we decided to randomly sample our data in order to compare statistically one data set to another. Hence, all the data sets were randomly sampled on the cross sections (points not located on cross sections were excluded) using the alea function of Excel 2010 to obtain $n = 630$. Frequency distributions of the bed elevation were plotted for all the data sets of $n = 630$ to assess the influence of vegetation development on the bar morphology (Bertoldi et al., 2011).

As initially proposed by Paola (1996) to study the transversal variability of shear stress in braided rivers and developed by Bertoldi et al. (2011) to describe the bed elevation frequency for bare and vegetated areas, we fitted a Γ density function:

$$p(H) = \frac{\alpha^{\alpha} H^{\alpha-1} e^{-\alpha H}}{\Gamma(\alpha)} \quad (1)$$

where H is the dimensionless bed elevation (elevation above the lowest point divided by the mean value), α describes the shape of the distribution, and Γ is the Euler gamma probability density function. As proposed by Bertoldi et al. (2011), the best fit value of α was obtained by minimizing the squared error between the measured data and data resulting from the Γ distribution.

2.4. Scour chains and grain size analysis

Scour-and fill-processes occurring on the bar were investigated using the scour chain method (Hassan, 1990; Laronne et al., 1994; Hassan et al., 1999; Laronne and Sholmi, 2007). Since 2008, 31 metal-linked chains were inserted vertically, anchored into the stream bed, and located in x, y, z axes using a DGPS. Scour chains were located on the above-mentioned cross sections (Fig. 1B) and distributed on morphological units 1 to 4 in order to link the annual topographical changes of the bar to the scour and fill processes. Each year, during low flows, scour chains were relocated by digging the bar sediments using the DGPS and a metal detector. The scoured and filled depths of bed material were determined on each chain by measuring the length of the chain above the elbow (maximum scour depth) and the distance between the elbow and the new bed level (subsequent sediment deposition).

Grain size analyses were performed using the standard method of dry sieving Ro-Tap on surface sediments sampled (in 2008, 2009, 2010, 2011, and 2012) at each scour chain location during insertion and relocation of scour chains. When armour layers were present, subsurface sediments were also sampled and analysed.

The critical bed shear stress was obtained using the Shields entrainment function (Shields, 1936):

$$\theta_c = \frac{\tau_c}{(\rho s - \rho w) g \cdot D} = fct \frac{u * D}{\nu} \quad (2)$$

where θ_c is the critical dimensionless shear stress, here taken as 0.047, τ_c is the critical boundary shear stress ($N \cdot m^{-2}$), ρ_s and ρ_w are (respectively) the density of sediment grains (2650 $kg \cdot m^{-3}$) and water (1000 $kg \cdot m^{-3}$), g is the acceleration due to gravity (9.81 $m \cdot s^{-2}$),

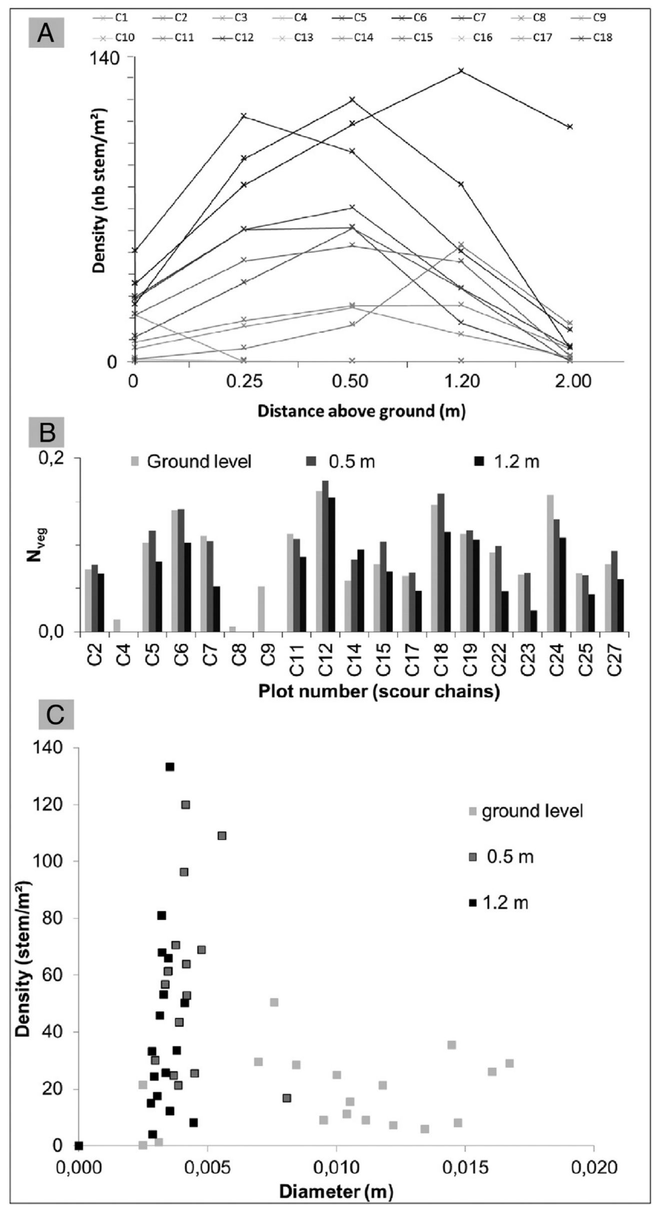

Fig. 3. (A) Number of stems and branches measured at 0, 0.25, 0.5, 1.2, and 2 m above the bed. (B) Manning's vegetation flow resistance parameter for each vegetated plot. (C) Relationship between tree diameter and number and stem/m².

and D is the grain diameter (here D_{10}, D_{50} and D_{90} in m); θ_c is a function of the Reynolds' grain number $Re_* = u^* D/v$, where u^* is the shear velocity ($m \cdot s^{-1}$) and v is the kinematic viscosity ($m^2 \cdot s^{-1}$).

For the higher magnitude flood of 2008, a dimentionless normalized excess bed shear stress (τ_{norm}) was calculated for the D_{10}, D_{50} and D_{90} parameters (before the flood) as follows:

$$\tau_{norm} D_{10} = \frac{\tau - \tau_{cD_{10}}}{\tau_{\max}} \tag{3}$$

$$\tau_{norm} D_{50} = \frac{\tau - \tau_{cD_{50}}}{\tau_{\max}} \tag{4}$$

$$\tau_{norm} D_{90} = \frac{\tau - \tau_{cD_{90}}}{\tau_{\max}} \tag{5}$$

where τ is the bed shear stress during the flood peak of 2008 ($2080\ m^3 \cdot s^{-1}$) calculated at each scour chain location; $\tau_{cD_{10}}$, $\tau_{cD_{50}}$, $\tau_{cD_{90}}$ are values of the critical bed shear stress for D_{10}, D_{50} and D_{90}, respectively; and $\tau_{\max}$ is the maximum value of τ reached on the bar during the flood (here $7.8\ N \cdot m^{-2}$).

The bed shear stress τ was obtained using the general equation:

$$\tau = \rho g R_h S \tag{6}$$

where τ is the bed shear stress ($N \cdot m^{-2}$), ρ is the density of water ($kg \cdot m^{-3}$), g is the acceleration of gravity ($m \cdot s^{-2}$), R_h is the hydraulic radius (taken here as water depth on each point during the flood obtained by subtracting the elevation each point to the water level during the flood [data from DREAL Centre], in m), S is the water surface slope (here taken as a constant $0.000226\ m \cdot m^{-1}$ [Latapie, 2011]).

2.5. Stratigraphical analysis of deposits

During summer 2012, four sections were dug on the bar for analysis of the sedimentary sequences at several scour chains locations and on the bank of two established islands (located near the bar studied [see Fig. 1] and 150 km downstream for comparison [see Détriché et al., 2010, for location]). For each section the stratigraphy of deposits was described in terms of thickness, bedding nature and orientation, and grain size; the elevation of each layer was recorded using a DGPS and sediments were collected for grain size analysis. The presence of thin silty and muddy dark layers rich in organic matter fragments and roots was noted. Such layers were shown by several previous studies carried out on the Loire (Rodrigues et al., 2006, 2007, 2012) to be suitable markers for emersion periods of the river bed.

2.6. Vegetation analysis

Woody vegetation patches present on the bar were mapped using a DGPS. Coefficients of cover-abundance (Braun-Blanquet, 1964; Fig. 1B) were determined in 2012 using the percentage of vegetation cover (Combroux et al., 2002) estimated from low-altitude aerial photographs and field observations.

Physical parameters of woody vegetation were analysed in 2012 to estimate its influence on flow resistance, sediment trapping, and retention. As performed by several authors (Kollmann et al., 1999; Rodrigues et al., 2006; Gilvear and Willby, 2006; Vreugdenhil et al., 2006; Corenblit et al., 2009) measurements were carried out on 4-m^2 plots centred on the scour chains. For each plot, stems originating from the bar surface were counted, and the size (height, diameter) of the five tallest and smallest trees was measured. The diameter of the five tallest and smallest trees was measured at, respectively, 1.2, 0.5, and 0 m from the bar surface.

The Manning's roughness parameter for each plot was calculated using the equation of Petryk and Bosmajian (1975) suitable for the areas covered with emerged vegetation:

$$n_{veg} = KnR_h{}^{2/3} \sqrt{\frac{C_d \sum Ai}{2gAL}} \tag{7}$$

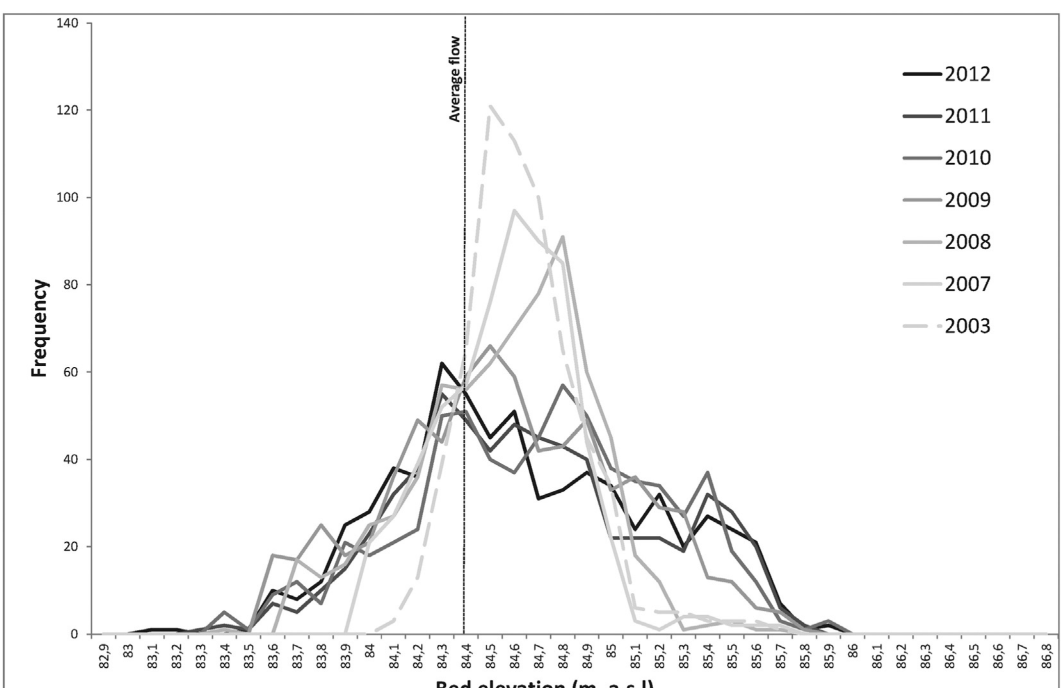

Fig. 4. Frequency of randomly sampled bed elevation from the years between 2003 and 2012 (n = 630 points). Data of 2003 correspond to the LiDAR data (courtesy of DREAL Centre) before vegetation development (2004). Data of surveys 2007 to 2012 correspond to field measurements.

Table 1
Kurtosis and skewness calculated on randomly sampled topographical data sets (n = 630 points).

	2003	2007	2008	2009	2010	2011	2012
Kurtosis	1.9	1.0	−0.1	−0.6	−0.5	−0.6	−0.7
Skewness	0.9	0.3	−0.3	0.0	−0.2	0.1	0.2

where n_{veg} is vegetation roughness, Kn is a factor of conversion equal to 1 for SI units, R_h is the hydraulic radius (in m), C_d is the drag coefficient (herein assumed to be equal to 1), ΣAi is the total frontal area of vegetation projected onto a plane perpendicular to the direction of flow (in m^2), g is the force of gravity (in m s^{-2}), A is the cross-sectional flow area (in m^2), L is unit length of the channel reach (in m).

The n_{veg} parameter, calculated for a unit surface of 1 m^2 has already been used by McKenney et al. (1995) on small streams in North America and by Rodrigues et al. (2006, 2007) on the Loire.

The computation of the n_{veg} roughness coefficients was performed using the physical parameters of the five tallest trees of each plot. The smallest trees, which were fully submerged and which tend to bend downstream during floods, were excluded from this analysis. Therefore, the n_{veg} parameters presented in this study refer to maximum roughness coefficients. Obviously, this corresponds to an approximation. Many studies have shown that pronated submerged plants do, in fact, contribute substantial roughness (for examples see Nepf and Ghisalberti, 2008; and Västilä et al., 2013).

3. Results

3.1. Typical stratigraphical architecture of island banks

On the Loire, the classical sedimentological architecture of islands presents two main units. A basal bar unit made of poorly sorted, sandy-gravelly sediments is observable on the lower part of trenches (Fig. 2). The stratae present in this unit are characterized by cross-bedding, by the presence of roots of former plants developed on the bar, and by thin layers (1 cm thick) of silt and mud intercalating with coarse sediments. This bar unit is overlaid by a relatively thin unit made of fine sediments (fine sands and silts, eventually mud) enriched in organic matter that can be compared to floodplain sediments transported as suspended load and deposited during flood events (Haschenburger and Cowie, 2009). Optically stimulated luminescence (OSL) datings done on one of these islands (Fig. 2A) shows that bar units can be rapidly deposited (2.5 m/14 y) compared to floodplain units, which correspond to lower sedimentation rates (1 m/192 y assuming that no vertical erosion occurred [see Détriché et al., 2010, for details]).

3.2. Pioneer woody vegetation developed on the bar

In 2012, the height of the pioneer trees ranged between 0.05 and 3.75 m.

For taller trees, a clear relationship is established between diameter and height. This trend is not perceptible for small trees. Some of them, relatively thick, are trees broken during floods or cut by beavers.

The density of the vegetation stands developed on the bar is significant and varies according to the distance from the bed (Figs. 3A and C).

The density of stems and branches (number/m^2) was often found to be at its maximum at 0.5 m above the bed; it decreased upward and downward. This explains the high values of vegetation resistance to flow (Fig. 3B). The high values of vegetation density at the elevation of 0.5 m can be explained by sprouting subsequent to tree breakage by flood flows or cutting by beavers.

3.3. Topographical and morphological evolution of the bar

Randomly sampled bar elevations measured between 2003 and 2012 were analysed in terms of frequency distribution (Fig. 4). The LiDAR data set of 2003 is characterized by a compact, unimodal, and rather symmetrical distribution. So in 2003 the bar was rather smooth with a mode equal to 84.5 m. After the establishment of pioneer vegetation (data sets of 2007 to 2012), the distribution displays smaller peaks and spreads. A similar process has been described for the Tagliamento River by Bertoldi et al. (2011). In the present study, smaller peaks of the distribution testify to the increased variability in bed elevation during time.

The shape of the distribution (Table 1) evolved from very leptokurtic (2003) to very platykurtic (2012). The skewness ranged between 0.9 and −0.3.

A shifting of the distribution toward the right during time highlights an aggradation process on the bar (Fig. 5). The development of the vegetation since 2004 modifies the rather simple pattern of the distribution that existed before its development. The α value, which varied between 1.9 and 13.8 (7.1 in average) is higher than proposed by Bertoldi et al. (2011) for the Tagliamento River.

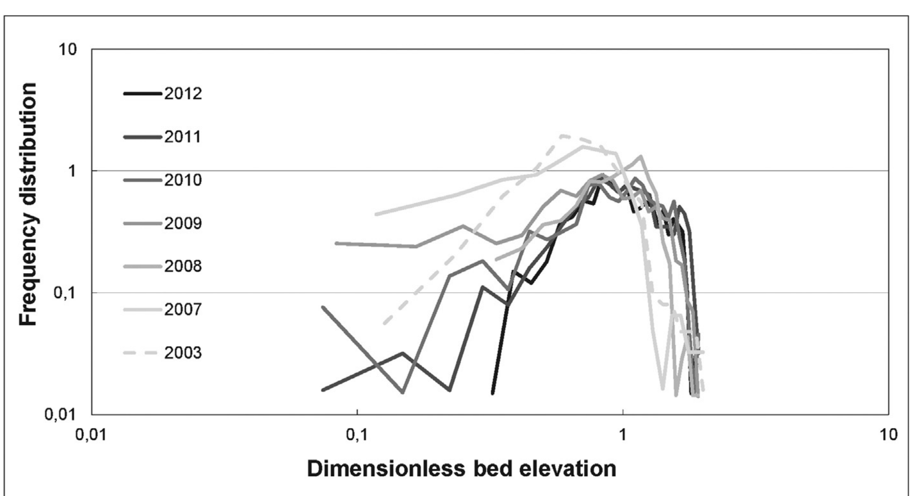

Fig. 5. Gamma function based on randomly sampled bed topography data between 2003 and 2012. Data of 2003 correspond to the liDAR data (courtesy of DREAL Centre) before vegetation development (2004). Data of surveys 2007 to 2012 correspond to field measurements.

Digital elevation models (Fig. 6) show a relatively plane surface of the bar in 2007 with superimposed low-amplitude longitudinal obstacle marks (Nakayama et al., 2002; Rodrigues et al., 2007; Euler and Herget, 2011; Euler et al., 2014) caused by the presence of patches of young trees.

The highest area of the bar was located at the upstream end of U1 (84.9 m asl) in 2007 and on U3 ($Z > 85$ m) in 2012. Between 2007 and 2012, the topographical contrast between units increased. Basically, the slope breaks on the margins of U1, U3 and U4 were reinforced, distinguishing each unit from U2.

On U1, most of the sediments were trapped because of the lee effect exerted by the upstream and higher part of this unit. In 2012, a significant sediment deposition occurred downstream of U1.

On U3, the merging of obstacle marks was accelerated by large volumes of coarse sediments coming from the main channel. The quantities of sediments deposited varied transversally during the survey

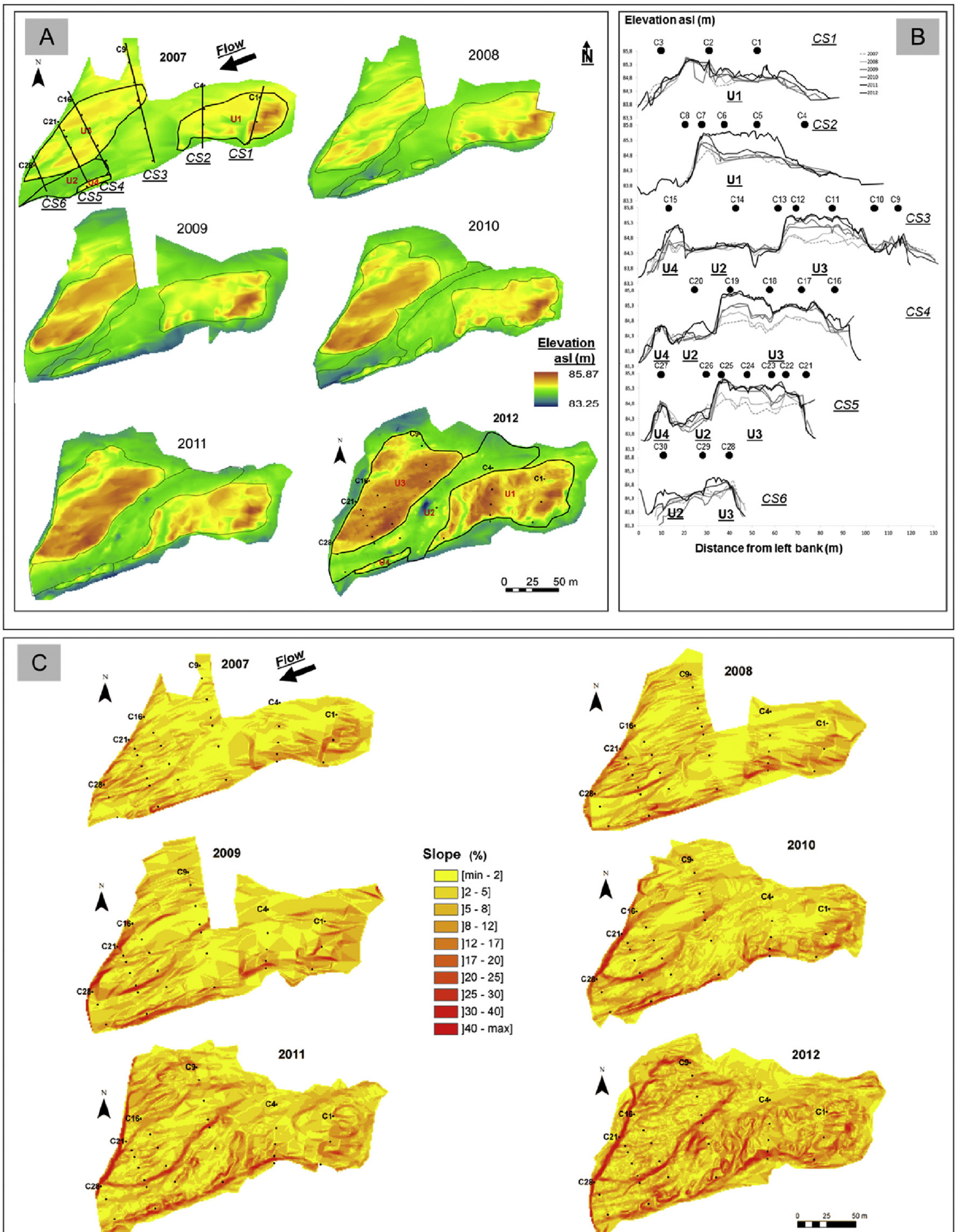

Fig. 6. Morphological evolution of the vegetated bar assessed from topographical surveys. Digital elevation models (DEMs) obtained on the bar (A), cross sections CS1 to CS6 with location of scour chains (C1 to C30) (B), and slope maps (C).

according to flood events (magnitude and duration). The low-amplitude ridge and swale topography of 2007 associated with obstacle marks evolved toward a higher, smoother, and well-defined unit. Between, 2010 and 2011, the longitudinal chute located in the downstream part was filled while another, separating U3 from an obstacle mark located at the north, appeared. The topographical survey also highlighted that steep slopes visible on the margins of U3 developed upstream between 2007 and 2012.

Changes in bed topography visible on U2 are relatively small compared to U1, U3, and U4. Although the upstream part of U2 is subject to scouring, this chute channel is stable in terms of elevation. The bed channel changes visible in the downstream part of the chute correspond to sediment by-passing.

The analysis of the cross sections (Fig. 6B) shows highly variable deposition rates over time in U3. On CS4 for instance, the left part of the bar did increase regularly in elevation except between 2009 and 2010. Conversely, a large quantity of sediment was deposited between 2008 and 2009 on the right part of the cross section.

The cross sections also show longitudinal evolution pattern of the bar margins as the increase of the slope of the banks shifted upstream during time. Comparing CS5, CS4, and CS3 shows that the asymmetry between the bar and the surrounding channels (namely U2 and the main channel located to the north) was higher on CS5 in 2007.

Since 2007, 8694 m^3 of sediments were deposited on the bar, while 4535 m^3 were eroded (Fig. 7). Hence, the budget between 2007 and 2012 was clearly positive (+4159 m^3). Fig. 7B shows the phasing of deposition of bedload sediments on CS2 to CS5. Between 2008 and 2009 (Fig. 7B), median elevation of CS4 and CS5 increased strongly highlighting a significant deposition on these two cross sections. Between 2009 and 2011, sediment deposition was higher on CS3. Between 2011 and 2012, median elevation of CS2 increased drastically caused by a large amount of sediments coming from upstream. These observations suggest that the deposition of sediments was directed upstream during the period surveyed.

The topographical surveys have shown that some areas of the bar were subject to erosion or deposition, only. In other words, these areas exhibited either a positive sediment budget (U1, U3, and U4) or a negative budget (U2 and the northern margin of U3) since 2007. The volumes of sediments trapped between 2007 and 2012 in the areas of continual deposition were estimated to 1023 m^3. The quantity of sediments trapped in the areas of continual deposition varied over time; between 2007–2008 and 2008–2009 it represented 25% of the sediments deposited on the whole bar, while it decreased to 15% between 2009 and 2010 and 16.5% between 2011 and 2012.

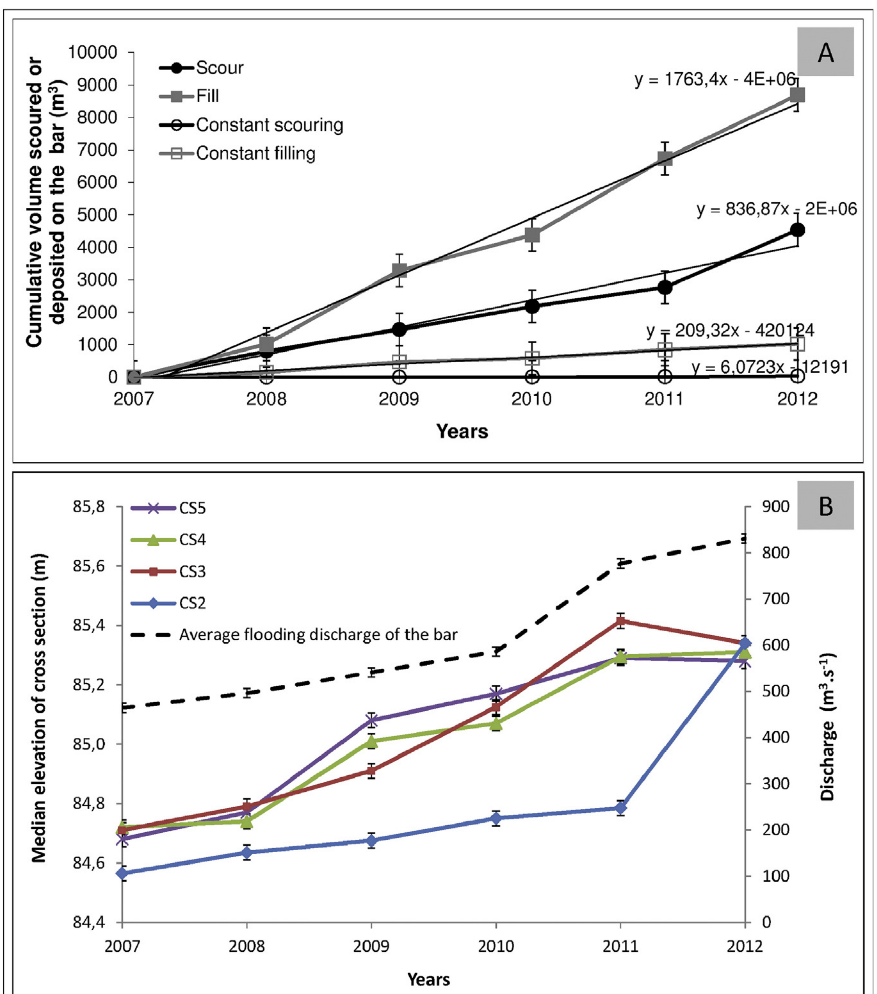

Fig. 7. (A) Cumulative curves of sediment deposition and scouring since 2007 on the entire bar (filled symbols) and on areas only affected by sediment deposition and erosion (empty symbols). (B) Median elevation (asl) of CS2 to CS5 and average value of the discharge able to inundate the bar.

3.4. Scour-and-fill processes on the bar

On the bar, the depth of scour decreased with time (Fig. 8). The maximum scour and/or fill depths recorded were about 0.8 m.

Morphological units 1, 3, and 4 were subject to sediment deposition, whereas scour was reduced because of the presence of vegetation. The morphological unit 2, bare subchannel, was characterized by intense sediment remobilization even if the average elevation did not change.

The analysis of several cross sections (Fig. 8) shows that the scour-and-fill processes varied according to the morphological units and their average elevation. In several places (e.g., scour chains C17, C24, and C25), a considerable accretion of sediment took place between 2008 and 2009, whereas no sediments were deposited after. This can be associated with the occurrence of a high-magnitude flood (Fig. 1). This is clearly different from what occurred in other places of the same morphological units where sediment deposition occurred progressively during time.

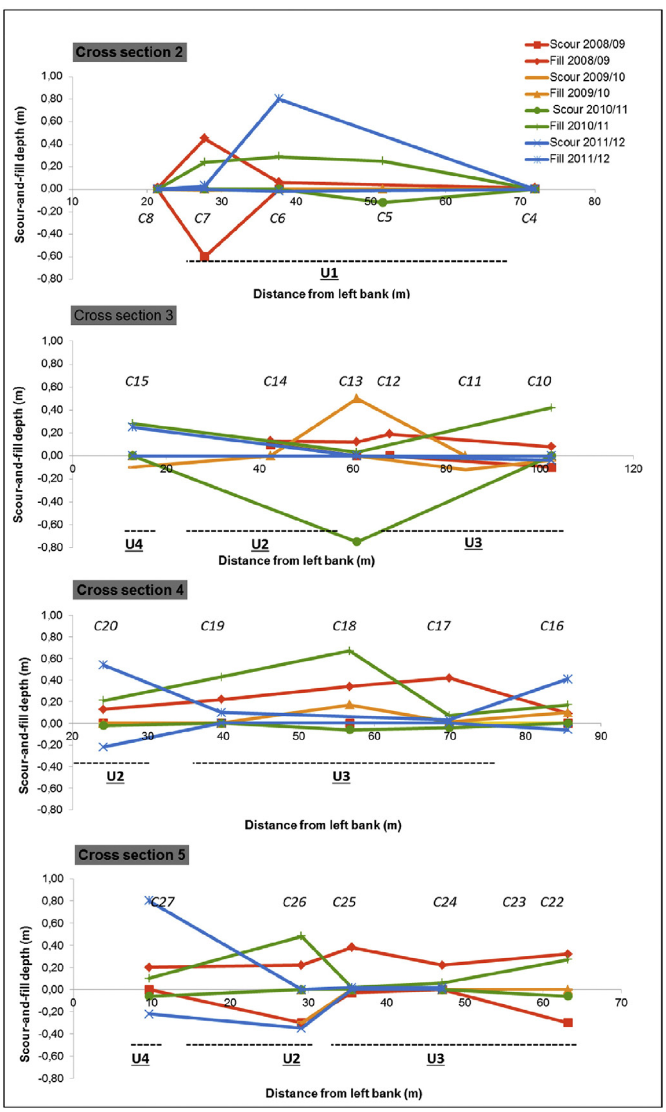

Fig. 8. Scour-and-fill depths recorded on cross Sections 2, 3, 4, and 5. Dashed lines correspond to morphological units on the mid-channel bar of Mareau-aux-Prés, and C4 to C27 correspond to the scour chain number.

3.5. Bar depositional architecture

Fig. 9 shows that the archiving of sediments on the bar was not continuous over time. For the same year, the archiving of sediments on the bar differed between morphological units considered (Rodrigues et al., 2012) depending on the presence or lack of vegetation. For instance, densely vegetated areas (C12, see Fig. 3B) were constantly characterized by vertical accretion of sediment that was rapidly fixed by tree roots.

Trenches show a classical general trend fining upward of sedimentary sequences. The internal structure consists mainly of poorly sorted bedload sediments at the base and planar cross-strata originating as a result of dune migration over the bar during flood events (e.g., upper parts of C6 and C15). Thin layers of fine sediments (mainly silts) enriched in organic matter and penetrated by roots are found in the densely vegetated areas (C12 and C22). These thin layers are markers of emersion phases and fixing of sediments by pioneer trees or herbs growing on obstacle marks (Rodrigues et al., 2007; Euler et al., 2014).

3.6. Grain size changes on the bar

Sediments present on the bar are mainly poorly sorted siliceous sands and gravels. Two populations of grains are clearly visible in Fig. 10A. Low-slope cumulative curves located in the right part of the graphs (Fig. 10A) correspond to very poorly sorted bedload sediments located in U2 or on the margins of vegetated areas. Higher-slope cumulative curves (on the left in graphs of Fig. 10A) were sampled in the vegetated morphological units, namely U1, U3, and U4. Comparison between years 2008–09, 2009–10, 2010–11, and 2011–12 shows a shift of the curves (Fig. 10A) toward the right for the low-slope cumulative curves and toward the left for the high-slope cumulative curves. This phenomenon indicates a fining of sediments trapped in the vegetation stands, while sediments located in the lower areas and on the margins of vegetation bands become generally coarser. For these areas, although the D_{90} remains constant, the whole mixture becomes coarser caused by the washing out of smaller grains downstream. This process leads to the development of armour layers on the margins of the vegetated areas.

Fig. 10B also shows that slope of cumulative curves of the sediments deposited in densely vegetated areas (namely C6, C12, and C22) increased during time. This indicates a better sorting and is explained by the increase of settling of suspended sediments as the vegetation developed and as mean elevation increased (less bedload sediments being deposited). In this case, the role played by vegetation on flow resistance and fine sediment settling is significant. If vegetation was absent, the intensity of fine sediment settling would not be so important.

The critical bed shear stress needed to entrain D_{50} and D_{90} particles was determined for all years between 2008 and 2012 (Fig. 11).

Depending on the grain size, the critical bed shear stress needed to initiate sediment motion ranges between 0.02 and 50.3 $N \cdot m^{-2}$. The latter value corresponds to large particles constituting armour layers present on the bar. For each year of comparison, the scatter of points increased and two groups of points can be identified. Points located above the bisector (larger grain size, higher critical bed shear stress) correspond to the sites located in U2 or on the margins of vegetated units, whereas points located below the bisector correspond mainly to vegetated areas.

3.7. Threshold for sediment motion vs vegetation

Table 2 and Fig. 12 compare the excess in bed shear stress responsible for sediment mobilization to the results of the scour-and-fill depths recorded in bare and vegetated areas.

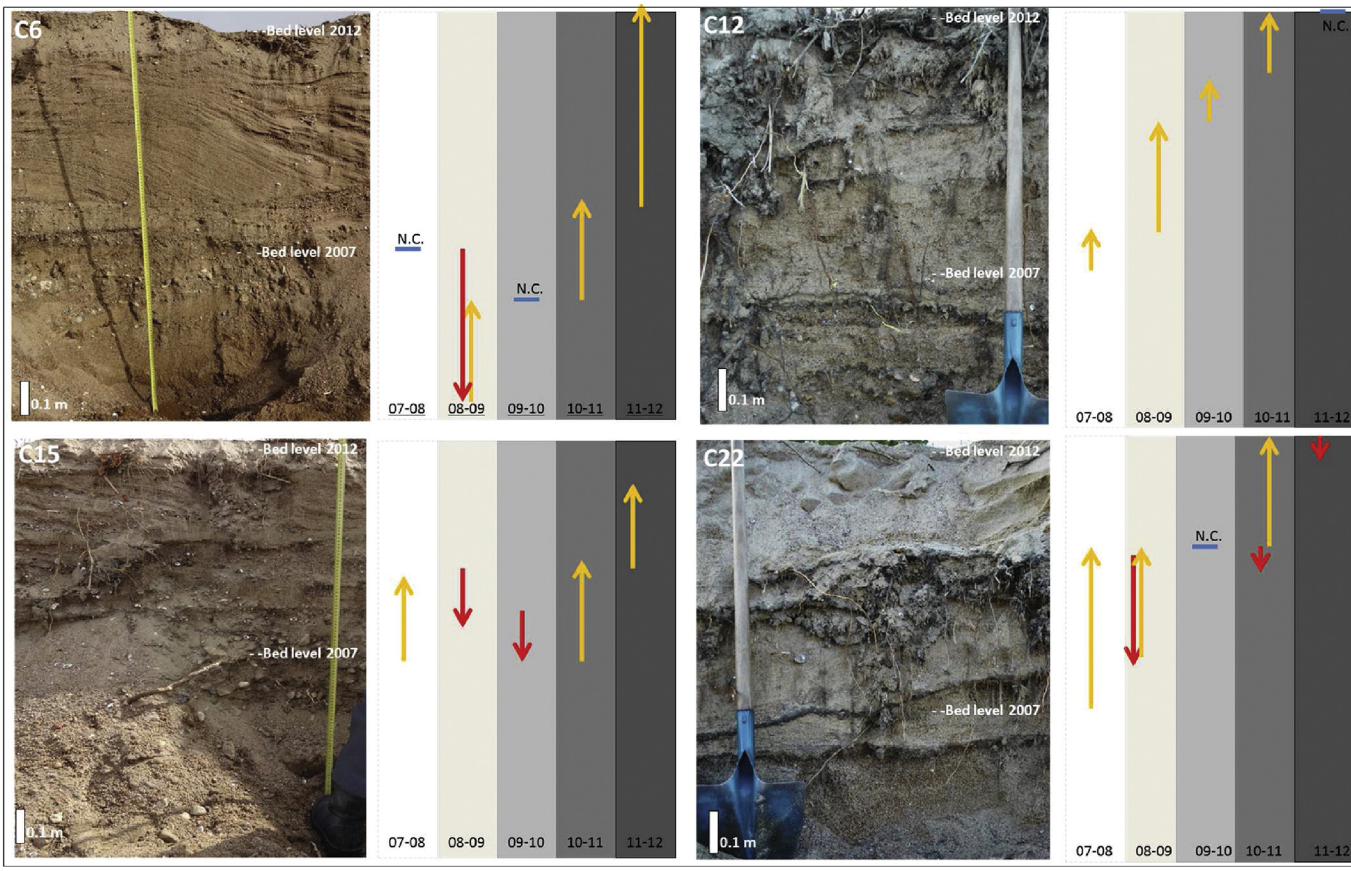

Fig. 9. Sediment architecture at four locations (representative of the morphological units of the bar) associated with scour-and-fill depths (arrows) measured using scour chains between 2008 and 2012. Results for year 2007 are based on topographical surveys only. Indication *N.C.* means no changes.

For bare areas, the normalized excess bed shear stress is in good agreement with the scour depth indicated by the scour chains (except for C10 and C8 where well-developed armour layers were present) as scouring occurred when excess bed shear stress was positive.

For vegetated areas, positive values of normalized excess bed shear stress are often associated with the lack of sediment scouring. This highlights the protection of sediments by the vegetation during flood events.

4. Discussion

4.1. Scour-and-fill processes during a flood are not directly interrelated to vegetation density or roughness parameter

The comparison between slightly and highly vegetated areas shows that the vegetation density or N_{veg} parameters are not correlated to the thickness of sediments deposited during the flood (Fig. 12). Owing to the fact that we calculated total boundary shear (not grain stress) making any meaningful conclusions about the relationship between shear stress, vegetation, and scour/fill is difficult. Anyway, the spatial distribution of sediment deposition clearly highlights the role played by the sediment supply on accretion of the bar during floods. This also suggests that other controlling factors are playing a role at a global scale (floods intensity–frequency–duration and associated sediment supply) and at a local scale (average elevation of the bar, bar surface form, deflection effect, sediment grain size).

4.2. Upstream-shifting accretion and grain-size segregation processes during first stages of island development

The topographical survey highlighted a change in the distribution of elevation of the bar during time (Figs. 4, 6, and 13A), evolving from very leptokurtic (2003) to very platykurtic (2012). In terms of morphology, the topography of the bar accreted and varied caused by the presence of obstacle marks. Fig. 13A steps 1, 2A, and 2B, shows the spreading of the distribution of elevations toward higher ones (dominant trend, from sediment trapping) and lower ones (because of scouring near the margins of tree bands).

The vertical accretion of the bar can be analysed at the local scale (tree band) and at the bar scale. At the local scale, sediment deposition results from the combination of two sedimentary processes. The first one corresponds to the development of obstacle marks growing downstream and laterally and is clearly visible on Fig. 6 for years 2007 and 2008. The second process corresponds to global deposition events at the bar scale (i.e., year 2009, see CS3 to 5 and U3 on Figs. 6 and 4; see also Wintenberger, 2011). Such events allowed sediment deposition in the space between previously existing obstacle marks. In other words, in the present study, obstacle marks developed principally when bedload supply was reduced, whereas large deposition events that highlight a significant bedload sediment supply coming from the main channel during the higher magnitude flood reached during the study period.

At the bar scale, the aggradation process apparently evolved in the upstream direction during time (Fig. 7B). We assume that the sediment deposition occurring in the downstream part of the bar results in backwater effect that facilitates sediment deposition immediately upstream during subsequent flood events. This regressive process led to the building of high-slope margins for U3 in the upstream direction between 2007 and 2012 (Fig. 6). The analysis of the median elevation of CS2 to CS5 shows that the presence of U3 contributed to a strong deflection of bedload sediment fluxes in 2012 that allowed significant sediment deposition on U2 (median elevation on CS2 being similar to the other cross sections; Fig. 7B). So

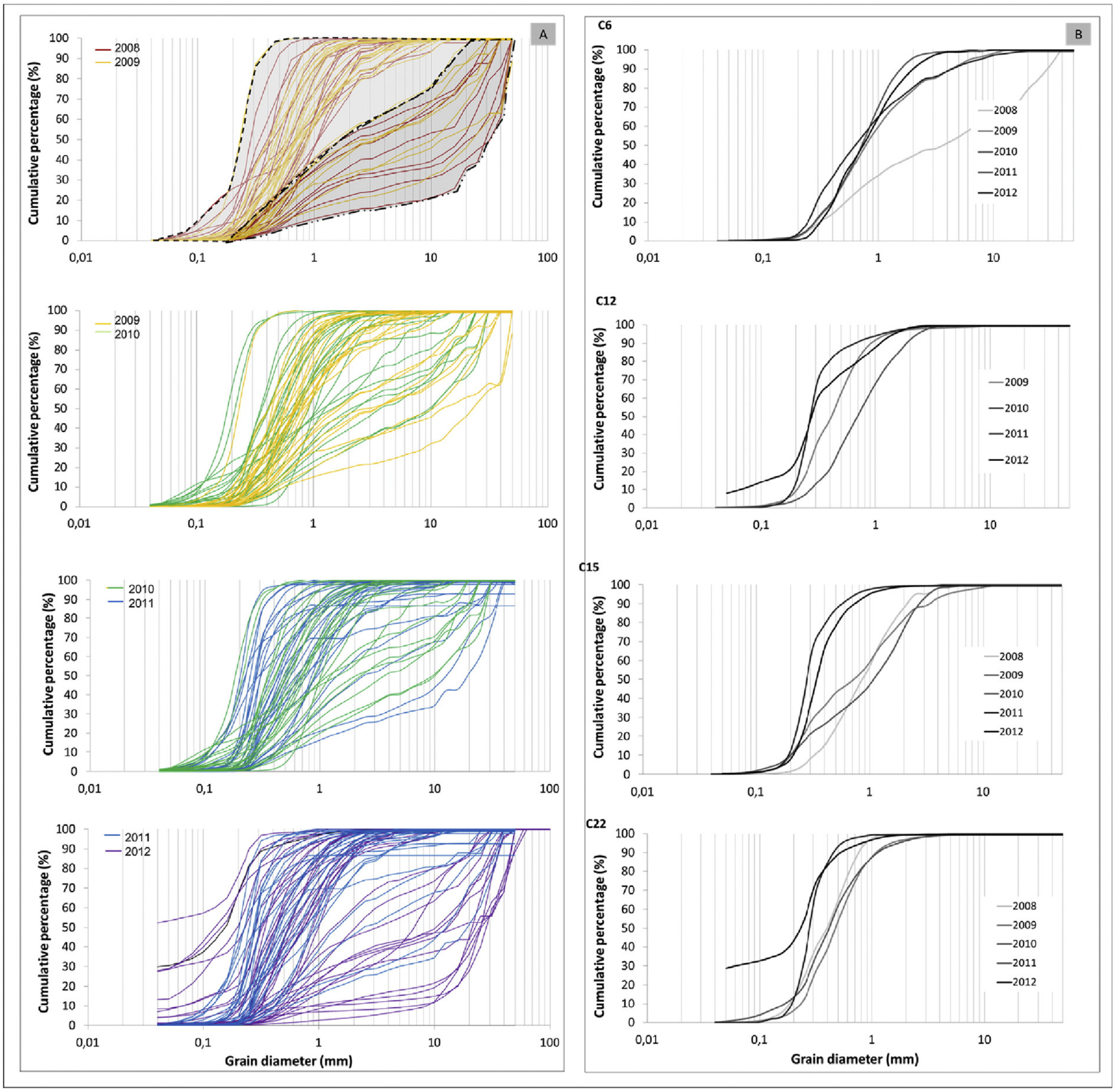

Fig. 10. (A) Grain-size evolution on the bar (all plots) between 2008 and 2012; note the two populations of grains on the first graph. (B) Grain size evolution at locations of trenches presented in Fig. 9. No data for C12 in 2008.

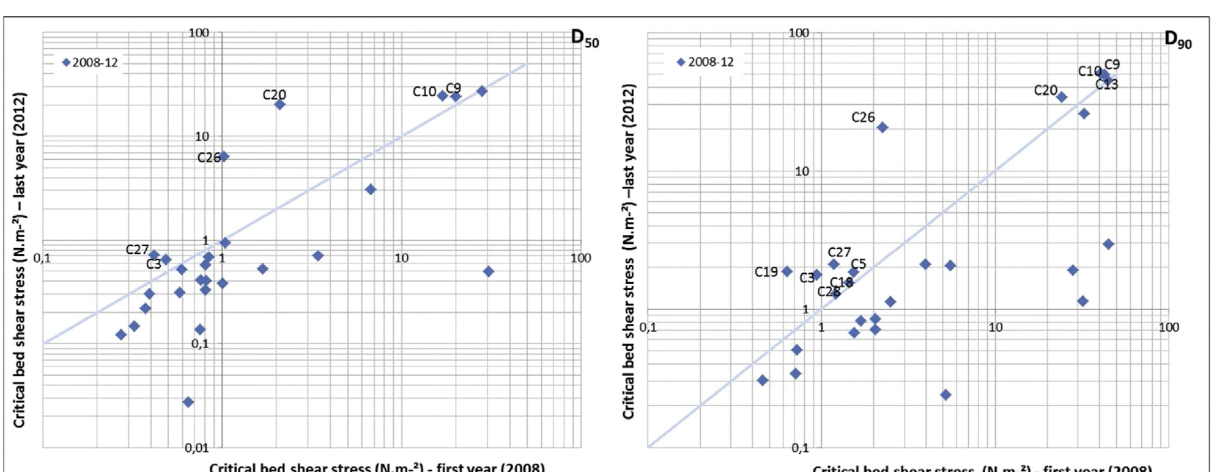

Fig. 11. Changes of the critical bed shear stress calculated for D_{50} (left graph) and D_{90} (right graph) of surface bar sediments between 2008 and 2012. The bisector indicates the same values of critical bed shear stress in both compared years. See Fig. 1 for location.

during the first stages after woody vegetation establishment, the accretion process seems to be principally governed by (i) space available between tree bands, (ii) bedload sediment supply, and (iii) vegetation type.

Generally, sediment sorting improved downstream. Segregation was observed between sediments surveyed on the vegetated and on the bare areas: the size of sediments trapped in the vegetation decreased (and their sorting increased), while sediments present in U2 or on the margins of the vegetated units get generally coarser (even if the D_{90} did not evolve significantly) mainly caused by the development of armour layers (Fig. 13B). This grain-size segregation process is a striking phenomenon that can be extrapolated to many sandy-gravelly fluvial systems. We assume here that the development of armoured layers as well as the general coarsening of sediments close to the vegetation bands can influence the incision process acting on surrounding channels. Comparing this study with the findings of Gurnell and Petts (2006) and Rodrigues et al. (2006), we suggest that the effect of vegetation on surrounding channels (deflection, turbulence) will differ according to the average grain size and the sorting of sediments. In sandy sites, incision of surrounding channels will be easier and not be significantly influenced by flow dynamics rather than sediment grain size. In sandy-gravelly sites, incision of surrounding channels will be slower because of this coarsening effect. As a consequence, the morphological evolution of developing islands and surrounding channels should be different (in terms of time response) for these two types of sites. Further investigations should be done in the future to detail this point.

The upward fining stratigraphical sequences observed for vegetated areas can be occasionally disturbed by deposition of coarser sediments during high-magnitude flood events (increase of bedload sediment supply). During these events, coarser sediments can be transported toward distal and high-elevation sites, and hence, intercalate with finer sediments. Even though sediments in the vegetated filter are relatively fine as a result of lower critical bed shear stress, they were not eroded during subsequent floods because of the high flow resistance. Specifically, the normalized excess bed shear stress associated with the flood of 2008 (higher magnitude flood event recorded) was not able to reach the threshold of sediment motion due to the vegetation presence (Table 2).

4.3. Conceptual model: from the vegetated bar state to the island state in low-gradient, sandy-gravelly rivers

Results presented in this paper hold for relatively large low-gradient, sandy-gravelly rivers and for pioneer vegetation from sexual regeneration. The study reach is characterized by an average specific stream power (22 $N \cdot Wm^{-2}$) smaller than the theoretical value of 30 $W \cdot m^{-2}$ described by Corenblit et al. (2009, 2014) and Francis et al. (2009) as the energy value allowing a durable biotic–abiotic reciprocal linkage.

Table 2
Normalized excess bed shear stress (for D_{10}, D_{50} and D_{90}) calculated for each scour chain for the flood of 2008 (2080 $m^3 \cdot s^{-1}$ at the gauging station of Orléans) compared to scour chain results between 2008 and 2009 and to the vegetation characteristics (density, stems$\cdot m^{-2}$ and N_{veg}).[a]

	Normalized excess bed shear stress			Scour / fill		Vegetation	
Location	$(\tau - \tau c_{D10})/\tau_{max}$	$(\tau - \tau c_{D50})/\tau_{max}$	$(\tau - \tau c_{D90})/\tau_{max}$	Scour	Fill	Density at 0.5 m	N_{veg} at 0.5 m
C1	0,7	-3,1	-5,0	-0,20	no data	0	0,000
C2	0,6	0,6	0,5	0,00	0,15	25,5	0,077
C3	0,9	0,9	0,8	-0,27	0,25	0	0,000
C4*	0,8	0,0	-3,3	0,00	0,01	0	0,000
C5*	0,7	0,6	0,5	0,00	0,00	70,5	0,116
C6	0,8	0,4	-2,8	0,00	0,06	96,25	0,142
C7	0,6	0,5	0,3	-0,60	0,45	61,5	0,104
C8*	1,0	0,9	0,3	0,00	0,00	0	0,000
C9*	0,7	-1,8	-4,7	no data	no data	0	0,000
C10*	0,8	-1,3	-4,4	-0,10	0,08	0	0,000
C11*	no data	no data	no data	no data	no data	53	0,106
C12	no data	no data	no data	0,00	0,19	109	0,176
C13*	0,8	-2,7	-4,8	0,00	0,12	0	0,000
C14*	no data	no data	no data	0,10	0,13	16,75	0,083
C15*	0,7	0,7	0,5	0,00	0,00	61,25	0,104
C16*	0,8	0,7	-3,2	0,00	0,09	0	0,000
C17	0,7	0,6	0,5	0,00	0,42	24,75	0,068
C18	0,8	0,7	0,7	0,00	0,34	120	0,159
C19	0,7	0,6	0,6	0,00	0,22	64	0,117
C20*	0,9	0,7	-2,2	0,00	0,13	0	0,000
C21	no data	no data	no data	no data	no data	0	0,000
C22	0,6	0,6	0,6	-0,30	0,32	56,75	0,099
C23	0,8	0,7	0,6	no data	no data	30	0,068
C24	0,7	0,6	0,0	0,00	0,22	69	0,129
C25	0,6	0,6	0,6	-0,03	0,38	21,25	0,065
C26	0,8	0,7	0,6	-0,30	0,22	0	0,000
C27	0,8	0,8	0,7	0,00	0,20	43,5	0,093
C28	0,7	0,7	0,6	-0,55	0,46	0	0,000
C29	0,8	0,7	0,6	-0,60	0,51	0	0,000
C30	1,0	0,9	0,5	-0,30	0,16	0	0,000

[a] For the normalized bed shear stress, light grey colour cells mean that sediments are theoretically in motion while dark grey cells mean no movement. For the vegetation, light grey colour cells correspond to bare areas, medium grey to small densities of trees (less than median) and dark grey to high densities of trees (more than median). The * indicated the presence of armour layer before the flood of 2008.

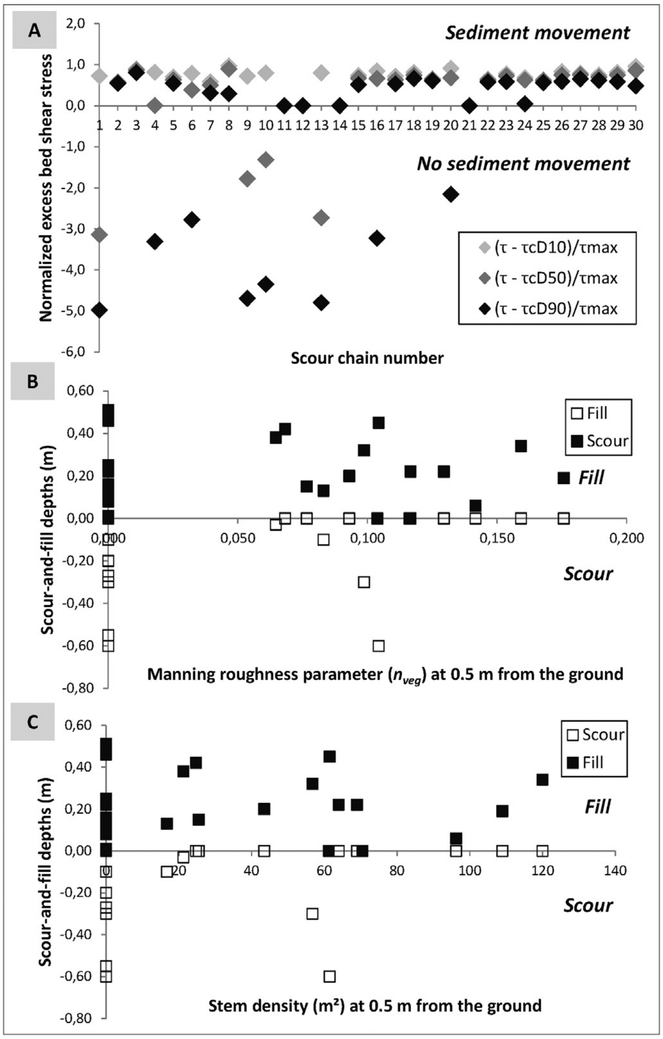

Fig. 12. Normalized excess bed shear stress and scour/fill depths observed and compared to the vegetation parameters (N_{veg}, stem density).

Rodrigues et al. (2007) suggested that this threshold value should be interpreted with care and modulated by the local physical and biological conditions. During the study period, the pioneer island was not renewed and a single trend to build a pioneer island occurred. This can be associated with the link between hydrology (several floods, occurred but the 2-year flood was only reached in 2008) and the biological traits of *P. nigra*, L. (Villar, 2011). During the study period (discharge did not reach high values), the small seedlings of *P. nigra* recruited in 2004 were able to withstand the physical stresses and rapidly influence their environment. This makes a strong difference compared to highly morphogical, highly active rivers such as braided rivers (e.g., Tagliamento see Van der Nat et al., 2002), where 30% of the islands are renewed every 2.5 years and island turnover takes between 12 and 24 years (Zanoni et al., 2008).

Scour chains and topographical surveys have shown nonlinear sediment archiving during the floods. Basically, sediment deposition rates are high during the first stages of development of vegetated bars, mainly influenced by the sediment supply (linked to the hydrology) coming from the main channel and by vegetation, which modulates scour and fill processes at local and bar scale (Fig. 13B, stage I). The spatial distribution of vegetation bands can influence the formation of obstacle and their ability to store sediments increasing the deflection power of the bands during subsequent floods. Tree cutting by beavers can result in sprouting of numerous shoots that will in turn increase their flow resistance. As aggradation is going on (Fig. 13B, stage II), the deflection of flow by the bar increases, and the sediment deposition rates decrease, caused by the fact that average elevation increases and inundation of the island becomes rare. Well known in literature, the deposition of bedload sediments decreases and is progressively replaced by settling of fine material transport as suspended load. However, during high-magnitude flood events, coarser sediments can be deposited on the fine sediments and then interbedded with these sediments. When the island is established (elevation is rather important and vegetation cover changed; Fig. 13B, stage III), fine sediment deposition occurs only during very high-magnitude (or exceptional) flood events. The low accretion rates during this step of island evolution and the deposition of autochthonous organic matter allows the building of the floodplain stratigraphical unit over decades (see Fig. 2). When the island banks are high, gravitational destabilization can occur, giving large quantity of sediments to the channel and then reducing the sediment volume stored in the island. During this step, riparian vegetation can stabilize the sediments on the banks or increase their erosion owing to surcharging (Fig. 13B, stage IIIb; Thorne, 1990). During stage IIIb, channel incision, changes in channel planform, and cattle activity can also trigger significant bank erosion. The trend is different for riprapped islands (Fig. 13B, stage IIIa).

5. Conclusions

The working hypothesis of this field study has been that nonmigrating (or forced) bars in relatively large and low-gradient, sandy-gravelly rivers can constitute a preferential area for woody vegetation recruitment and survival. The feedback exerted by the black poplar (*P. nigra*, L.) on these bars can trigger a rapid evolution toward an island form. Detailed field surveys of one of these nonmigrating bars of the Loire River lead us to the following conclusions:

- The dense vegetation bands trapped and fixed sediments during floods and induced a specific signature on topography and grain-size (which evolved during the study period, Fig. 13A).
- A combination of two deposition processes was identified: (i) generation of obstacle marks in the downstream direction leading to (ii) a global regressive accretion of the bar and development of well-defined margins prefiguring the future island banks.
- The morphological changes noted on the bar were controlled by the bedload sediment supply coming from the main channel deflected by the previously established tree bands.
- The development of tree bands triggers a grain-size segregation (finer sediments in the vegetated areas vs. generally coarser sediments in the surrounding channels), which is assumed to influence the timing of disconnection between a growing island and the surrounding channels, specifically in gravelly sites.
- The use of a normalized excess bed shear stress parameter showed that the fixing of sediments is significantly influenced by the characteristics of vegetation, whereas the amount of sediments deposited during the flood is not directly related to vegetation density or roughness parameter.
- The conceptual model proposed in this study suggests that the archiving of sediments and the morphological changes are rapid during the first stage of development of a vegetated bar whereas because the bar is high enough to be submerged only during high-magnitude floods, it slowly evolves toward an island form. In relatively large sandy-gravelly rivers, woody pioneer vegetation significantly increases the preservation potential of sediments leading to quasi-continuous sediment deposition rates.

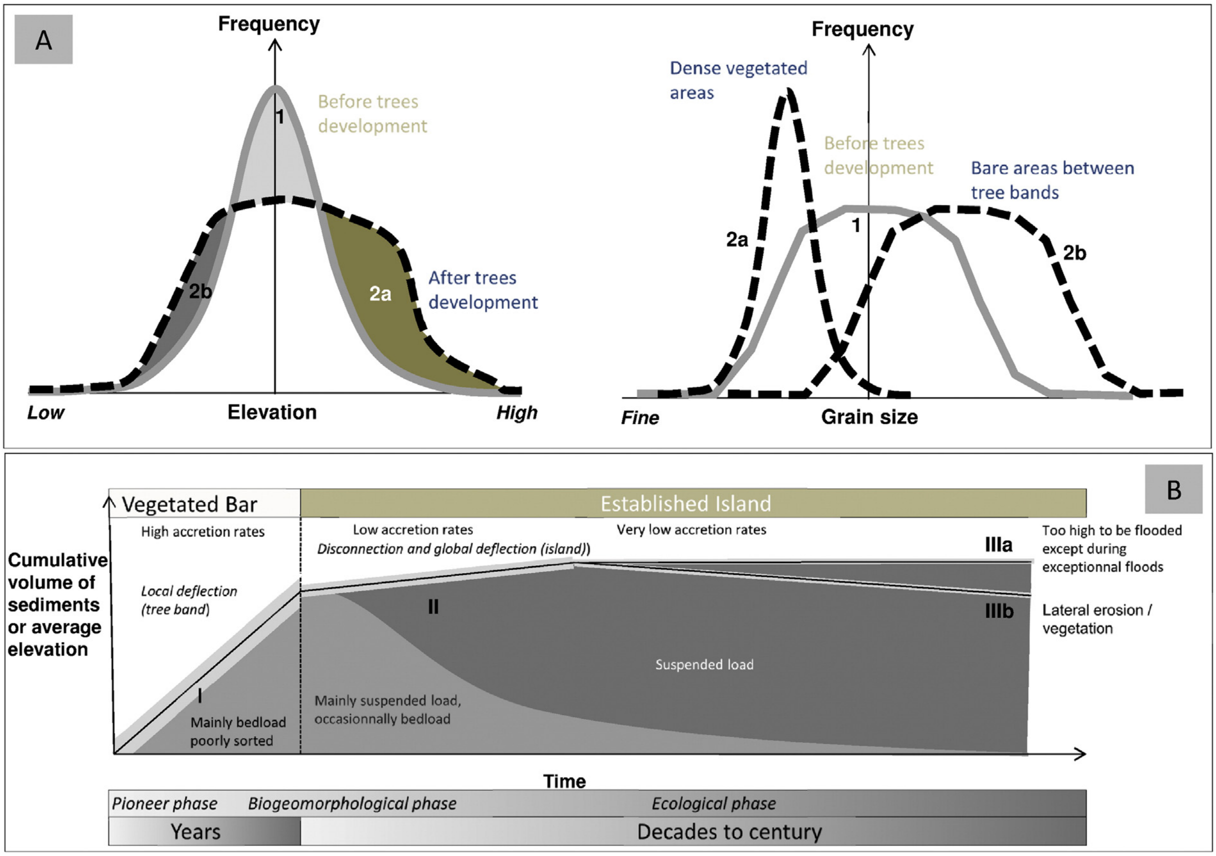

Fig. 13. (A) Conceptual model of evolution from a vegetated bar to an established island state. Consequences of the first stages of development of pioneer trees on topography and grain size during years following colonization. (B) Transition (longer time scale) between a vegetated bar and an established island. Comparison is made with the fluvial biogeomorphological succession of Corenblit et al. (2014).

Acknowledgements

This study constitutes the main part of the Master Thesis in Geosciences of the second author defended in 2011. The paper was written jointly by the first two authors, and this work was initiated by the second author in 2007; it recently benefited from support from the Masterplan Plan Loire Grandeur Nature (BioMareau Project, FEDER (Presage n°37729)/Région Centre/INRA (DR-RD 27), Coord. M. Villar).

The authors wish to thank J.P. Bakyono, R. Delancret, B. Deleplancque, H. El Abida, L. Gouny, P. Jugé, M. Lemay, I. Pene, M. Rincel (University F. Rabelais — Tours) for their valuable field assistance and analytical operations. M. Chantereau and D. Hemeray (Réserve naturelle de St Mesmin) are thanked for their support and interest. C. Pasquier (Inra Orléans) is also acknowledged for her help during topographical measurements in summer 2009. W. Bertoldi (University of Trento) is warmly thanked for his advice during the analysis of topographical results. The authors are grateful to the reviewers and the chief editor for their useful comments that improved the paper.

References

Abbe, T.B., Montgomery, D.R., 2003. Patterns and processes of wood debris accumulation in the Queets river basin, Washington. Geomorphology 51, 81–107.
Antonarakis, A.S., Richards, K.S., Brasington, J., Muller, E., 2010. Determining leaf area index and leafy tree roughness using terrestrial laser scanning. Water Resour. Res. 46, W06510.
Bertoldi, W., Gurnell, A.M., Drake, N., 2011. The topographic signature of vegetation development along a braided river: results of a combined analysis of airborne lidar, colour air photographs and ground measurements. Water Resour. Res. 47, W06525.
Braun-Blanquet, J., 1964. Flanzensoziologie, Grundzüge der Vegetationskunde. 3rd ed. Springer-Verlag, Wien.
Brice, J.C., 1964. Channel patterns and terraces of the Loup River in Nebraska. U.S. Geological Survey Prof. Paper, 422D pp. 1–41.
Bridge, J.S., 2003. Rivers and Floodplains: Forms, Processes, and Sedimentary Record. Blackwell, Oxford (ISBN 978-0-632-6489-2, 491 pp.).
Charron, I., Johnson, E.A., Martin, Y.E., 2011. Tree establishment on bars in low-order gravel-bed mountain streams. Earth Surf. Process. Landf. 36, 1522–1533.
Claude, N., Rodrigues, S., Bréhéret, J.-G., Bustillo, V., Jugé, P., 2014. Interactions between flow structure and morphodynamics of migrating bars in a channel widening/narrowing of the Loire river (France). Water Resour. Res. http://dx.doi.org/10.1002/2013WR015182.
Combroux, I., Bornette, G., Amoros, C., 2002. Plant regenerative strategies after a major disturbance: the case of a riverine wetland restoration. Wetlands 22, 234–245.
Copeland, R.R., 2000. Determination of Flow Resistance Coefficients due to Shrubs and Woody Vegetation. US army corps of engineers (ERDC/CHL HETN-II-3, 8 pp.).
Corenblit, D., Steiger, J., Gurnell, A.M., Tabacchi, E., Roques, L., 2009. Control of sediment dynamics by vegetation as a key function driving biogeomorphic succession within fluvial corridors. Earth Surf. Process. Landf. 34, 1790–1810.
Corenblit, D., Baas, A.C.W., Bornette, G., Darrozes, J., Delmotte, S., Francis, R.A., Gurnell, A.M., Julien, F., Naiman, R.J., Steiger, J., 2011. Feedbacks between geomorphology and biota controlling Earth surface processes and landforms: a review of foundation concepts and current understandings. Earth Sci. Rev. 106, 307–331.
Corenblit, D., Steiger, J., González, E., Gurnell, A.M., Charrier, G., Darrozes, J., Dousseau, J., Julien, F., Lambs, L., Larrue, S., Roussel, E., Vautier, F., Voldoire, O., 2014. The biogeomorphological life cycle of poplars during the fluvial biogeomorphological succession: a special focus on *Populus nigra* L.
Crosato, A., Mosselman, E., Desta, F.B., Uijttewaal, W.S.J., 2011. Experimental and numerical evidence for intrinsic nonmigrating bars in alluvial channels. Water Resour. Res. 47, W03511.
Crouzy, B., Edmaier, K., Pasquale, N., Perona, P., 2013. Impact of floods on the statistical distribution of riverbed vegetation. Geomorphology 202, 51–58.
Dacharry, M., 1996. Les grandes crues historiques de la Loire. La Houille Blanche 6 (7), 47–53.
Darby, S.E., Simon, A., 1999. Incised River Channels. Processes, Forms, Engineering and Management. Wiley, Chichester (442 pp.).
Détriché, S., Rodrigues, S., Macaire, J.J., Bonté, P., Bréhéret, J.G., Bakyono, J.P., Juge, P., 2010. Caesium-137 in sandy sediments of the River Loire (France): assessment of an alluvial island evolving over the last fifty years. Geomorphology 115, 11–22.
Dhivert, E., Grosbois, C., Rodrigues, S., Desmet, M., 2015. Influence of fluvial environments on sediment archiving processes and temporal pollutant dynamics (upper Loire River, France). Sci. Total Environ. 505, 121–136.

Drago, E.C., Wantzen, K.M., Paira, A.R., 2008. The Lower Paraguay river-floodplain habitats in the context of the Fluvial Hydrosystem Approach. Ecohydrol. Hydrobiol. 8 (1), 49–66.

Duband, D., 1996. La genèse des crues dans le bassin de la Loire. La Houille Blanche 6 (7), 54–62.

Euler, T., Herget, J., 2011. Obstacle-Reynolds-number based analysis of local scour at submerged cylinders. J. Hydraul. Res. 49, 267–271.

Euler, T., Herget, J., 2012. Controls on local scour and deposition induced by obstacles in fluvial environments. Catena 91, 35–46.

Euler, T., Zemke, J., Rodrigues, S., Herget, J., 2014. Influence of inclination and permeability of solitary woody riparian plants on local hydraulic and sedimentary processes. Hydrol. Process. 28, 1358–1371.

Fathi-Maghadam, M., Kouwen, N., 1997. Nonrigid, nonsubmerged, vegetative roughness on floodplains. J. Hydraul. Eng. 123, 51–57.

Fielding, C.R., Alexander, J., Newman-Sutherland, E., 1997. Preservation of in-situ, arborescent vegetation and fluvial bar construction in the Burdekin River of north Queensland, Australia. Palaeogeogr. Palaeoclimatol. Palaeoecol. 135, 123–144.

Francis, R.A., Gurnell, A.M., Petts, G.E., Edwards, P.J., 2006. Riparian tree establishment on gravel bars: interactions between plant growth strategy and the physical environment. In: Sambrook Smith, G.H., Best, J.L., Bristow, C.S., Petts, G.E., Jarvis, I. (Eds.), Braided Rivers: Process, Deposits, Ecology and ManagementInternational Association of Sedimentologists Special Publication vol. 36. Blackwell, Malden, MA, pp. 361–380.

Francis, R., Corenblit, D., Edwards, P., 2009. Perspectives on biogeomorphology, ecosystem engineering and self-organisation in island-braided fluvial ecosystems. Aquat. Sci. 71, 290–304.

Freeman, G.E., Rahmeyer, W.H., Copeland, R.R., 2000. Determination of Resistance due to Shrubs and Woody Vegetation. US Army corps of engineers (ERDC/CHL TR 00-25, 33 pp.).

Fuller, I.C., Hutchinson, E., 2007. Sediment flux in a small gravel-bed stream: response to channel remediation works. N. Z. Geogr. 63, 169–180.

Gautier, E., Grivel, S., 2006. Multi-scale analysis of island formation and development in the Middle Loire River, France, In J.S. Rowan, R.W. Duck, A. Werrity, sediment dynamics and the hydromorphology of fluvial systems. IAHS Publ. 306, 179–187.

Gibling, M.R., Davies, N.S., 2012. Palaeozoic landscapes shaped by plant evolution. Nat. Geosci. 5, 99–105.

Gibling, M.R., Davies, N.S., Falcon-Lang, H.J., Bashforth, A.R., DiMichele, W.A., Rygel, M.S., Ielpi, A., 2014. Palaeozoic co-evolution of rivers and vegetation: a synthesis of current knowledge. Proc. Geol. Assoc. 125 (5–6), 524–533.

Gilvear, D., Willby, N., 2006. Channel dynamics and geomorphic variability as controls on gravel bar vegetation; river Tummel, Scotland. River Res. Appl. 22, 457–474.

Graf, W.L., 1978. Fluvial adjustments to the spread of tamarisk in the Colorado Plateau region. Geol. Soc. Am. Bull. 89, 1491–1501.

Grosbois, C., Meybeck, M., Lestel, L., Lefèvre, I., Moatar, F., 2012. Severe and contrasted polymetallic contamination patterns (1900–2009) in the Loire River sediments (France). Sci. Total Environ. 435–436, 290–305.

Gurnell, A.M., Petts, G.E., 2006. Trees as riparian engineers: the Tagliamento river, Italy. Earth Surf. Process. Landf. 31, 1558–1574.

Gurnell, A.M., Petts, G.E., Hannah, D.M., Smith, B.P.G., Edwards, P.J., Kollmann, J., Ward, J.V., Tockner, K., 2001. Riparian vegetation and island formation along the gravel-bed Fiume Tagliamento, Italy. Earth Surf. Process. Landf. 26, 31–62.

Gurnell, A.M., Tockner, K., Edwards, P.J., Petts, G.E., 2005. Effects of deposited wood on biocomplexity of river corridors. Front. Ecol. Environ. 3 (7), 377–382.

Gurnell, A.M., Bertoldi, W., Corenblit, D., 2012. Changing river channels: the roles of hydrological processes, plants and pioneer fluvial landforms in humid temperate, mixed load, gravel bed rivers. Earth Sci. Rev. 111, 129–141.

Haschenburger, J.K., Cowie, M., 2009. Floodplain Stages in the Braided Ngaruroro River, New Zealand. 103 pp. 466–475.

Hassan, M.A., 1990. Scour, fill, and burial depth of coarse material in gravel bed streams. Earth Surf. Process. Landf. 15, 341–356.

Hassan, M.A., Schick, A.P., Shaw, P.A., 1999. The transport of gravel in an ephemeral sandbed river. Earth Surf. Process. Landf. 24, 623–640.

Heritage, G.L., Milan, D.J., Large, A.R.G., Fuller, I.C., 2009. Influence of survey strategy and interpolation model on DEM quality. Geomorphology 112, 334–344.

Ielpi, A., Gibling, M.R., Bashforth, A.R., Lally, C., Rygel, M.C., Al-Silwadi, S., 2014. Role of Vegetation in Shaping Early Pennsylvanian Braided Rivers: Architecture of the Boss Point Formation, Atlantic Canada. http://dx.doi.org/10.1111/sed.12109.

Kollmann, J., Vieli, M., Edwards, P.J., Tockner, K., Ward, J.V., 1999. Interactions between vegetation development and island formation in the Alpine river Tagliamento. Appl. Veg. Sci. 2, 25–36.

Laronne, J.B., Sholmi, Y., 2007. Depositional character and preservation potential of coarse-grained sediments deposited by flood events in hyper-arid braided channels in the Rift Valley, Arava, Israel. Sediment. Geol. 195, 21–37.

Laronne, J.B., Outhet, D.N., Carling, P.A., McCabe, T.J., 1994. Scour chain employment in gravel bed rivers. Catena 22, 299–306.

Latapie, A., 2011. Modélisation de l'évolution morphologique d'un lit alluvial: application à la Loire moyenne (PhD thesis), University of Tours — Irstea (277 pp.).

Latapie, A., Camenen, B., Rodrigues, S., Moatar, F., Paquier, A., 2014. Assessing channel response of a long river influenced by human disturbance. Catena 121, 1–12.

Li, R.M., Shen, H.W., 1973. Effect of tall vegetations on flow and sediment. J. Hydraul. Div. 99, 793–814.

Manners, R.B., Schmidt, J.C., Scott, M.L., 2014. Mechanisms of vegetation-induced channel narrowing of an unregulated canyon river: results from a natural field-scale experiment. Geomorphology 211, 100–115.

McKenney, R., Jacobson, R.B., Wertheimer, R.C., 1995. Woody vegetation and channel morphogenesis in low gradient, gravel-bed streams in the Ozark Plateaus, Missouri and Arkansas. Geomorphology 13, 175–198.

Mikuś, P., Wyżga, B., Kaczka, R.J., Walusiak, E., Zawiejska, J., 2013. Islands in a European mountain river: linkages with large wood deposition, flood flows and plant diversity. Geomorphology 202, 115–127.

Moggridge, H.L., Gurnell, A.M., 2009. Controls on the sexual and asexual regeneration of Salicaceae along a highly dynamic, braided river system. Aquat. Sci. 71, 305–317.

Moore, I.D., Grayson, R.B., Ladson, A.R., 1991. Digital terrain modelling: a review of hydrological, geomorphological, and biological applications. Hydrol. Process. 5, 3–30.

Nakayama, K., Fielding, C.R., Alexander, J., 2002. Variations in character and preservation potential of vegetation-induced obstacle marks in the variable discharge Burdekin River of north Queensland, Australia. Sediment. Geol. 149, 199–218.

Nanson, G.C., Knighton, A.D., 1996. Anabranching rivers: their cause, character and classification. Earth Surf. Process. Landf. 21, 217–239.

Nepf, H., Ghisalberti, M., 2008. Flow and transport in channels with submerged vegetation. Acta Geophys. 56 (3), 753–777.

Olesen, K.W., 1984. Alternate bars in and meandering of alluvial rivers. In: Elliott, C.M. (Ed.), River Meandering, Proc. Conf. Rivers 1983. ASCE, New Orleans, pp. 873–884 (1984).

Osterkamp, W.R., 1998. Processes of fluvial island formation, with examples from Plum Creek, Colorado and Snake river, Idaho. Wetlands 18, 530–545.

Paola, C., 1996. Incoherent structure: turbulence as a metaphor for stream braiding. In: Ashworth, P.J., Bennett, S.J., Best, J.L., Mc Lelland, S.J. (Eds.), Coherent Flow Structures in Open Channels. John Wiley and Sons, pp. 706–723.

Parker, G., Johanneson, H., 1989. Observations on several recent theories of resonance and overdeepening in meandering channels. In: Ikeda, S., Parker, G. (Eds.), River meandering, Water Resources Monograph 12, pp. 379–415.

Petryk, S., Bosmajian, G., 1975. Analysis of flow through vegetation. J. Hydraul. Div. 101, 871–884.

Reinfelds, I., Nanson, G., 1993. Formation of braided river floodplains, Waimakariri River, New Zealand. Sedimentology 40, 1113–1127.

Rodrigues, S., Bréhéret, J.G., Macaire, J.J., Moatar, F., Nistoran, D., Jugé, P., 2006. Flow and sediment dynamics in the vegetated secondary channels of an anabranching river: the Loire River (France). Sediment. Geol. 186, 89–109.

Rodrigues, S., Bréhéret, J.G., Macaire, J.J., Greulich, S., Villar, M., 2007. In-channel woody vegetation controls on sedimentary processes and the sedimentary record within alluvial environments: a modern example of an anabranch of the River Loire (France). Sedimentology 54, 223–242.

Rodrigues, S., Claude, N., Jugé, P., Bréhéret, J.G., 2012. An opportunity to connect the morphodynamics of alternate bars with their sedimentary products. Earth Surf. Process. Landf. 37, 240–248.

Rodrigues, S., Mosselman, E., Claude, N., Wintenberger, C., Juge, P., 2015. Alternate bars in a sandy gravel bed river: generation, migration and interactions with superimposed dunes. Earth Surface Processes and Landforms 40 (5), 610–628.

Shields, A., 1936. Anwendung der Aehnlichkeitsmechanik und der Turbulenzforschung auf die Geschiebebewegung. Mitteilung der Preussischen Versuchsanstalt fur Wasserbau und Schiffbau, Berlin (26 pp.).

Struiksma, N., Olesen, K.W., Flokstra, C., de Vriend, H.J., 1985. Bed deformation in curved alluvial channels. J. Hydraul. Res. 23 (1), 57–79.

Tal, M., Paola, C., 2007. Dynamic single-thread channels maintained by the interaction of flow and vegetation. Geology 35, 347–350.

Thorne, C.R., 1990. Effects of vegetation on riverbank erosion and stability. In: Thornes, J.B. (Ed.), Vegetation and Erosion: Processes and Environments. Wiley, New York, pp. 125–144.

Tubino, M., 1991. Growth of alternate bars in unsteady flows. Water Resour. Res. 27, 37–52.

Tubino, M., Repetto, R., Zolezzi, G., 1999. Free bars in rivers. J. Hydraul. Res. 37, 759–775.

Van der Nat, D., Schmidt, A.P., Tockner, K., Edwards, P.J., Ward, J.V., 2002. Inundation dynamics in braided floodplains (Tagliamento River, northeast Italy). Ecosystems 5, 636–647.

Västilä, K., Järvelä, J., Aberle, J., 2013. Characteristic reference areas for estimating flow resistance of natural foliated vegetation. J. Hydrol. 492, 49–60.

Villar, M., 2011. Conservation des ressources génétiques du peuplier noir dans son habitat: bases biologiques, génétiques et écologiques. Habilitation Dissertation (112 pp.).

Vreugdenhil, S.J., Kramer, K., Pelsma, T., 2006. Effects of flooding duration, frequency and depth on the presence of saplings of six woody species in north-west Europe. For. Ecol. Manag. 236, 47–55.

Wende, R., Nanson, G.C., 1998. Anabranching rivers: ridge-form alluvial channels in tropical northern Australia. Geomorphology 22, 205–224.

Wintenberger, C., 2011. Transformation d'une barre sédimentaire de la Loire Moyenne en île: influence de la végétation ligneuse (Master's Thesis), University of Tours (50 pp.).

Wu, F.C., Shen, H.W., Chou, Y.J., 1999. Variation of roughness coefficients for unsubmerged and submerged vegetation. J. Hydraul. Eng. 125, 934–942.

Zanoni, L., Gurnell, A.M., Drake, N., Surian, N., 2008. Island dynamics from analysis of historical maps and air photographs. River Res. Appl. 24, 1141–1159.